Malaysian Journal of Microbiology, Vol 22(1) 2026, pp. 97-105
DOI: http://dx.doi.org/10.21161/mjm.240825

Malaysian Journal of Microbiology
Published by Malaysian Society for Microbiology
(In SCOPUS since 2011)

Assessment of antibacterial activity in TiO_2@SiO_2-modified graphitic carbon nitride nanomaterials

Estefanny Sonia Ngalih, Devagi Kanakaraju, Hung Hui Chung and Micky Vincent*

Faculty of Resource Science and Technology, Universiti Malaysia Sarawak, 94300 Kota Samarahan, Sarawak, Malaysia.
Email: vmicky@unimas.my

Received 24 September 2024; Received in revised form 2 October 2025; Accepted 3 February 2026

ABSTRACT

Aims: The aim of this study was to evaluate the antibacterial properties of a TiO_2-SiO_2/g-C_3N_4 nanocomposite synthesised using sol-gel and thermal polymerisation methods.
Methodology and results: Field-Emission Scanning Electron Microscopy (FE-SEM) and Energy Dispersive X-ray (EDX) analyses were used to characterise the surface topology of the nanocomposite. The antibacterial efficacies of the synthesised TiO_2-SiO_2/g-C_3N_4 were assessed through agar well diffusion, disk diffusion, and broth macrodilution (minimum inhibitory concentration, MIC) assays. The test microorganisms included two bacterial species: *Escherichia coli* and *Staphylococcus aureus*. No visible zones of inhibition (ZOIs) were observed in either the agar well or disk diffusion assays, likely due to limited diffusion, poor solubility, and the short-lived nature of reactive oxygen species (ROS). However, MIC testing in liquid media revealed notable antibacterial activity, with MIC values of 0.25% for *E. coli* and 1.0% for *S. aureus*. This was further corroborated by SEM analysis, which revealed significant morphological damage in both bacterial species, underscoring the antibacterial potential of the TiO_2-SiO_2/g-C_3N_4 nanocomposite.
Conclusion, significance and impact of study: Results suggest that TiO_2-SiO_2/g-C_3N_4 nanocomposite demonstrated effective antibacterial activity through ROS-mediated mechanisms, particularly under aqueous conditions that facilitate close contact with bacterial cells. These findings highlight its potential as a versatile agent for controlling bacterial contamination, especially in applications such as wastewater treatment, where moist environments enhance photocatalytic performance.

Keywords: Antibacterial activity, reactive oxygen species, TiO_2-SiO_2/g-C_3N_4 nanocomposite, wastewater treatment

INTRODUCTION

Waterborne infections caused by microorganisms affect millions of lives annually, primarily due to inadequate water treatment and lack of access to clean water in many parts of the world (Edokpayi *et al.*, 2018). It is estimated that 361,000 children under the age of five die each year from diarrhea caused by waterborne diseases such as hepatitis A, cholera, and typhoid fever (Magana-Arachchi and Wanigatunge, 2020). The risk of waterborne disease outbreaks persists when sanitation and water treatment are insufficient. Although deaths from diarrheal illnesses are more prevalent in economically disadvantaged regions, numerous cases are still reported in developed nations, where water treatment infrastructures are more advanced (Griffiths, 2008). Concerns over contaminated water supplies have led to efforts to find practical and cost-effective disinfection methods.

Chlorination has been the most common method of water treatment since the early 1900s (Nielsen *et al.*, 2022). However, this approach has been associated with the formation of mutagenic and carcinogenic by-products, raising safety concerns (Qadafi *et al.*, 2023). Additionally, research indicates that chlorine, at concentrations typically used in water treatment, is not fully effective against certain microorganisms. These include spore-forming bacteria such as *Bacillus* species, highly chlorine-tolerant organisms such as *Cryptosporidium* spp. and *Giardia lamblia*, and yeasts such as *Clavispora lusitaniae* (Al-Abri *et al.*, 2019; Gupta *et al.*, 2022). These limitations underscore the need for alternative methods that are economically viable, effective, and safe. One such method is photocatalysis.

Photocatalysis has gained attention due to its potential for water decontamination using direct sunlight. According to Byrne *et al.* (2015), semiconductors like titanium dioxide (TiO_2) can act as photocatalysts, absorbing light and catalysing water and oxygen to generate reactive

*Corresponding author

ISSN (print): 1823-8262, ISSN (online): 2231-7538

Malays. J. Microbiol. Vol 22(1) 2026, pp. 97-105
DOI: http://dx.doi.org/10.21161/mjm.240825

oxygen species. These highly active oxidants are capable of inactivating microorganisms, making TiO_2 a promising antibacterial agent for water treatment applications. However, earlier studies have shown that pristine TiO_2 exhibits weak photocatalytic performance under visible light, which may limit its effectiveness against waterborne microbes (Etacheri *et al.*, 2015). To address this drawback, TiO_2 is often combined with other semiconductors to enhance its photocatalytic properties, expand its absorption band gap, and reduce the likelihood of electron-hole recombination in nanostructures (Etacheri *et al.*, 2015; Moma and Baloyi, 2018).

A recent innovation in TiO_2-based nanocomposites for water treatment combines TiO_2, silica (SiO_2), and graphitic carbon nitride (g-C_3N_4) (Wu *et al.,* 2016). According to Dong *et al.* (2014) and Kumar *et al.* (2018), g-C_3N_4 is a novel organic polymer-like semiconductor with excellent catalytic properties, a stable structure, and the ability to be excited by visible light due to its narrow optical band gap of about 2.7 eV. While this nanocomposite has been used for treating organic chemical pollutants, research on its antibacterial properties remains limited. Therefore, this study assesses the antibacterial activity of the TiO_2-SiO_2/g-C_3N_4 composite against the Gram-negative bacterium *Escherichia coli* and the Gram-positive bacterium *Staphylococcus aureus* using agar well diffusion, disk diffusion, broth macrodilution, minimum inhibitory concentration (MIC), and morphological analysis via scanning electron microscopy (SEM).

MATERIALS AND METHODS

Materials and nanocomposite preparation

All reagents used in this study were of analytical grade and utilized without further purification. The nanocomposite was prepared using commercially available materials from various suppliers. Commercial anatase TiO_2, tetraethyl orthosilicate (TEOS, 98%) as the SiO_2 precursor, and urea (99.5%) as the g-C_3N_4 precursor were obtained from Sigma-Aldrich (Steinheim, Germany). Ethanol (95.0%) was purchased from HmBG (Selangor, Malaysia), and hydrochloric acid (HCl, 36.5-38.0%) was acquired from J.T. Baker (Thailand). Deionised water (Sartorius Arium®, Kuala Lumpur, Malaysia) was used in the preparation of all solutions.

Synthesis of silica (SiO_2) nanoparticles

SiO_2 nanoparticles were synthesised using the sol-gel method. Initially, 22.2 mL of TEOS was added to 29.2 mL of ethanol with vigorous stirring. Subsequently, 7.2 mL of deionised water and 0.4 mL of 37% HCl were added, and the solution was stirred for 15 min. The mixture was then heated in a water bath at 90 °C for 1 h until the solvent evaporated, resulting in the formation of brittle, white SiO_2. The SiO_2 was then ground and subjected to calcination in a furnace (Carbolite Type 301, United Kingdom) at 500 °C for 3 h.

Synthesis of graphitic carbon nitride (g-C_3N_4) nanoparticles

g-C_3N_4 nanoparticles were synthesised via thermal polymerisation. A 10 g quantity of urea was placed into a ceramic crucible, covered with a lid and aluminium foil, and heated in a furnace at 550 °C for 3 h. The resulting yellow product was then sonicated (Daihan Scientific Co., Ltd., South Korea) with 1 L of deionised water for 2 h, centrifuged five times at 3000 rpm for 10 min each, and subsequently washed five times with deionised water using vacuum filtration through a 0.45 µm membrane filter. The product was then dried overnight in an oven (Memmert, Germany) at 70 °C and ground into fine particles.

Synthesis of TiO_2-SiO_2/g-C_3N_4 nanocomposite

The TiO_2-SiO_2/g-C_3N_4 nanocomposite was synthesised by mixing the prepared SiO_2 and g-C_3N_4 with commercial anatase TiO_2 in a 1:1:1 ratio in 100 mL of deionised water under continuous magnetic stirring for 2 h. The resulting mixture was transferred into a ceramic crucible and subjected to a hydrothermal process at 150 °C for 5 h. After the hydrothermal treatment, the resulting light-yellow compound was filtered using vacuum filtration through a 0.45 µm membrane filter to separate the solid product, and subsequently dried at 100 °C for 2 h.

Analysis of synthesised nanocomposite

The synthesised nanocomposite was analysed using Field-Emission Scanning Electron Microscopy and Energy Dispersive X-ray (FESEM-EDX) (JEOL JSM-IT500HR, Japan). FESEM was employed to determine the morphology and capture the microstructure of TiO_2-SiO_2/g-C_3N_4, while EDX was used to determine the chemical composition of the nanocomposite.

Preparation of nanocomposite suspensions

A 1.0% (w/v) nanocomposite suspension was prepared by dissolving 1.0 g of TiO_2-SiO_2/g-C_3N_4 in 100 mL of 0.85% saline solution to produce the original stock solution. The stock solution was then diluted with 0.85% saline solution to create additional nanocomposite suspensions at concentrations of 0.75%, 0.50%, and 0.25% (w/v).

Bacterial cultures and inoculum preparation

Escherichia coli and *S. aureus* were selected as representative Gram-negative and Gram-positive bacterial strains, respectively, due to their clinical relevance and distinct structural characteristics. This selection enabled comparative evaluation of the nanocomposite's antibacterial activity across two major bacterial classes. Both bacterial cultures were obtained from Microbiology Laboratory 2 of the Faculty of

 ISSN (print): 1823-8262, ISSN (online): 2231-7538

Malays. J. Microbiol. Vol 22(1) 2026, pp. 97-105
DOI: http://dx.doi.org/10.21161/mjm.240825

Resource Science and Technology, University of Malaysia Sarawak (UNIMAS). The bacterial stock cultures were grown on nutrient agar (Merck KGaA, Germany). These cultures were confirmed through macroscopic characterisation (colony morphology) and microscopic observation of Gram-stained smears. Inocula were then prepared by culturing and diluting the stock cultures in nutrient broth (Merck KGaA, Germany) to achieve the desired concentrations.

Determination of antibacterial activity of synthesised TiO_2-SiO_2/g-C_3N_4

Agar well diffusion

The agar well diffusion assay, a rapid and qualitative method, was used to determine the antibacterial activity of the nanocomposite. Bacterial strains were adjusted to a turbidity equivalent to the 0.5 McFarland standard, achieving cell densities of approximately 10^8 CFU/mL, using spectrophotometric absorbance at 625 nm (Shimadzu, Malaysia). A 100 µL aliquot of the adjusted bacterial suspension was spread aseptically onto the surface of nutrient agar using a sterile cotton swab. Five 6 mm wells were created in each plate using a cork borer, and 150 µL of nanocomposite suspensions at different concentrations (0.25%, 0.50%, 0.75%, 1.0%) were added to the wells. A well containing 150 µL of 0.85% saline solution served as the negative control. No positive control was included, as the focus of this study was to evaluate the intrinsic antibacterial activity of the TiO_2-SiO_2/g-C_3N_4 nanocomposite without comparison to standard antibiotics. The plates were incubated under visible light at 37 °C for 24 h. The zones of inhibition (ZOI) were measured using a caliper, and the results were recorded in millimetres. Each treatment was performed in triplicate for each bacterium, and mean results were calculated.

Disk diffusion

The antibacterial activity of TiO_2-SiO_2/g-C_3N_4 was further evaluated using the disk diffusion method, based on the procedure described by Kirby Bauer (Bauer *et al.*, 1966). Bacterial strains were adjusted to a turbidity equivalent to the 0.5 McFarland standard (approximately 10^8 CFU/mL) using spectrophotometric absorbance at 625 nm. Sterile blank antimicrobial susceptibility disks were used in the test, with four disks loaded with 10 µL of nanocomposite suspension at concentrations of 0.25%, 0.50%, 0.75%, and 1.0%, respectively. The fifth disk containing 10 µL of 0.85% saline solution acted as a negative control. As in the agar well diffusion assay, no positive control was included, as the focus of this study was to evaluate the intrinsic antibacterial activity of the TiO_2-SiO_2/g-C_3N_4 nanocomposite without comparison to standard antibiotics. The disks were then placed on the agar plates and incubated under visible light at 37 °C for 24 h. The zones of inhibition (ZOI) were measured with a caliper in millimetres. Each experiment was conducted in triplicate for each bacterium, and the mean results were calculated.

Broth microdilution

The Minimum Inhibitory Concentration (MIC) of TiO_2-SiO_2/g-C_3N_4 was determined using a macrodilution assay, following the guidelines of the Clinical and Laboratory Standards Institute (CLSI, 2015). The MIC test was performed in seven 4 mL round-bottomed centrifuge tubes. Bacterial strains were adjusted to the turbidity of the 0.5 McFarland standard, achieving cell densities of approximately 10^8 CFU/mL using spectrophotometric absorbance at 625 nm. 2 mL of 1.0% TiO_2-SiO_2/g-C_3N_4 were serially diluted two-fold in 0.85% saline solution, after which 2 mL of bacterial strains were added to tubes 3 through 7. Tube 1 served as a positive control, containing only 4 mL of 1.0% TiO_2-SiO_2/g-C_3N_4, while tube 2 served as a negative control (no treatment), containing 4 mL of medium inoculated with bacterial strains. The tubes were vortexed to mix the solutions thoroughly and incubated under visible light at 37 °C for 24 h. MIC values were determined by comparing the initial (0 h) and final (24 h) absorbance at 600 nm (OD_{600}), a standard wavelength for estimating bacterial growth in broth cultures. According to Wacogne *et al.* (2024), OD_{600} provides a reliable, non-destructive measure of cell density by maximising light scattering from bacterial cells while minimising interference from cellular absorption and the coloration of growth media. The MIC was defined as the lowest concentration of TiO_2-SiO_2/g-C_3N_4 that inhibited bacterial growth. Each sample concentration for each bacterium was tested in triplicate, and the mean absorbance values was reported.

Morphological analysis of microorganisms using scanning electron microscopy (SEM)

Scanning Electron Microscopy (SEM) (JEOL JSM-IT500HR, Japan) was used to examine the morphological changes in bacterial strains treated with TiO_2-SiO_2/g-C_3N_4 nanocomposite. Samples were prepared using the MIC samples from the broth macrodilution method and untreated bacterial cells. 2 mL of the MIC sample and 2 mL of untreated bacterial inoculum were transferred into separate 2 mL centrifuge tubes and centrifuged at 1000 rpm for 10 min. Centrifugation was employed to accelerate the separation of particles based on size, shape, density, and medium viscosity (Singh *et al.*, 2015). To obtain clear SEM images, the resulting pellets were washed with deionised water 3 to 5 times using centrifugation at 3000 rpm for 10 min to remove impurities. The pellets were then air-dried in an incubator (Tambi-160, India) at 37 °C overnight. After drying, the samples were coated with a fine layer of gold using an auto-fine gold coater (JEOL, Japan) for 5 min. The coated samples were then analysed under SEM to observe any morphological changes.

Statistical analysis

 ISSN (print): 1823-8262, ISSN (online): 2231-7538

Malays. J. Microbiol. Vol 22(1) 2026, pp. 97-105
DOI: http://dx.doi.org/10.21161/mjm.240825

All experiments were conducted in triplicate for each bacterium. Data were analysed using the Statistical Package for Social Sciences (SPSS) version 22.0 (IBM Corp, Illinois, USA). A one-way analysis of variance (ANOVA) was performed, and descriptive statistics, including mean and standard deviation, were calculated. Post-hoc comparisons were carried out using Tukey's test to assess the significance of differences between MICs. A value of $p < 0.05$ was considered statistically significant.

RESULTS AND DISCUSSION

This study aimed to evaluate the antibacterial effects of a synthesised TiO_2-SiO_2/g-C_3N_4 nanocomposite. The nanocomposite was analysed using Field-Emission Scanning Electron Microscopy and Energy Dispersive X-ray (FESEM-EDX) to determine its size, shape, and surface topology, all of which are critical factors influencing its antibacterial properties. Figure 1 presents the FESEM analysis of the morphology of individual nanoparticles and the TiO_2-SiO_2/g-C_3N_4 nanocomposite at 10,000× magnification. As shown in Figure 1(A), the commercial anatase TiO_2 appeared spherical and exhibited good dispersion, though the particles tended to clump together, consistent with previous findings by Kanakaraju *et al.* (2021). The synthesised SiO_2, depicted in Figure 1(B), exhibited irregular, crystal-like structures with sharp angles, reflecting the characteristics described by Wardani *et al.* (2023). The g-C_3N_4 particles, shown in Figure 1(C), displayed a layered, flaky structure. This morphology is likely due to the use of urea as a precursor, which releases volatile gases such as water (H_2O) and hydrogen sulphide (H_2S) during synthesis. These gases contribute to the formation of microporous inorganic nanocrystals within the g-C_3N_4 framework and the exfoliation of carbon nitride sheets, leading to a more wrinkled and irregular appearance, as noted by Sareshkeh *et al.* (2023). In comparison, the TiO_2-SiO_2/g-C_3N_4 nanocomposite, shown in Figure 1(D), appeared as a heterogeneous compound with distinct particle sizes and shapes. The TiO_2 particles were heavily agglomerated on the surface of SiO_2, while g-C_3N_4 was scattered among the TiO_2 and SiO_2 particles. This configuration is likely to result in a high surface area and the presence of multiple active sites, enhancing the nanocomposite's potential antibacterial activity.

The successful synthesis of TiO_2-SiO_2/g-C_3N_4 nanocomposite was further verified through Energy Dispersive X-ray (EDX) analysis, which was used to determine the elemental composition of each compound in the individual nanoparticles and the TiO_2-SiO_2/g-C_3N_4 nanocomposite, as shown in Table 1. The EDX analysis of TiO_2 revealed an atomic composition of 29.96% titanium (Ti) and 70.04% oxygen (O), approximating the expected stoichiometric ratio of 1:2. For the synthesised SiO_2, the EDX results confirmed the formation of silica with an atomic composition of 23.48% silicon (Si) and 76.52% oxygen (O). The analysis of g-C_3N_4 showed an atomic composition of 38.14% carbon (C) and 61.86% nitrogen (N), reflecting the expected stoichiometric ratio of 1:2. In the TiO_2-SiO_2/g-C_3N_4 nanocomposite, the EDX analysis revealed atomic compositions of 0.33% titanium (Ti), 0.30% silicon (Si), 74.71% carbon (C), and 24.66% oxygen (O), indicating successful integration of the components. However, nitrogen (N) was not detected, likely due EDX detection limits or its low concentration relative to other elements. Rades *et al.* (2014) and Guyett *et al.* (2024) noted that light elements such as nitrogen often fall below EDX detection thresholds due to their low atomic number, weak X-ray emission, and susceptibility to peak overlaps and background interference—particularly when present in trace amounts or embedded within complex matrices. Therefore, the absence of detectable nitrogen does not necessarily indicate its absence in the material.

The antibacterial activity of the TiO_2-SiO_2/g-C_3N_4 nanocomposite was evaluated against two bacterial species: *E. coli* and *S. aureus*. The results of the agar well diffusion, disk diffusion, and minimum inhibitory concentration (MIC) assays are summarized in Table 2. In the agar well diffusion and disk diffusion methods, suspensions of the nanocomposite were either introduced into wells cut into agar plates inoculated with the test

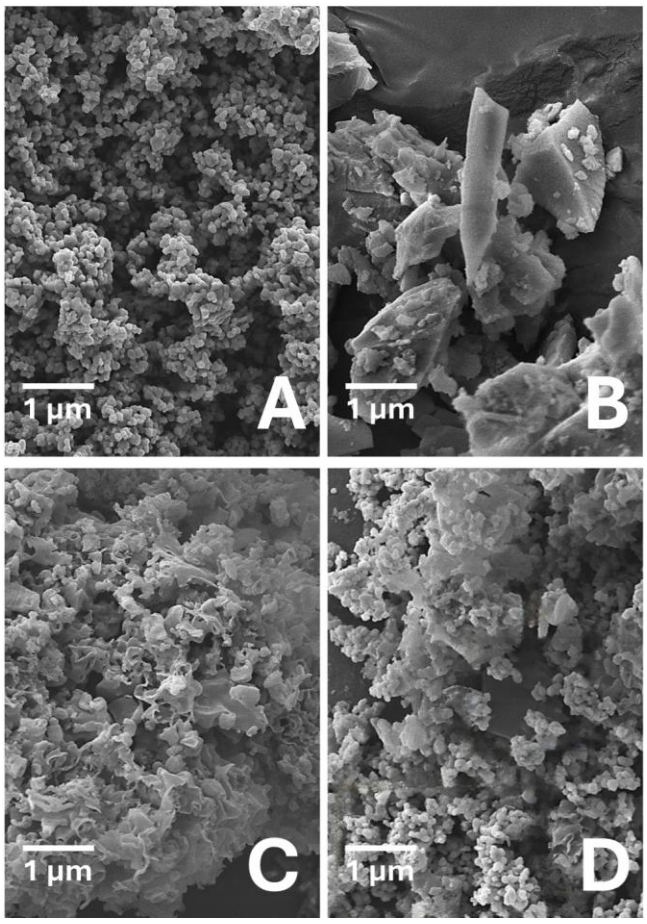

Figure 1: FE-SEM results with 10,000X magnification: (A) Titanium dioxide (TiO_2), (B) Silica (SiO_2), (C) Graphitic

 ISSN (print): 1823-8262, ISSN (online): 2231-7538

Malays. J. Microbiol. Vol 22(1) 2026, pp. 97-105
DOI: http://dx.doi.org/10.21161/mjm.240825

carbon nitride (g-C_3N_4) and (D) TiO_2/SiO_2/g-C_3N_4 nanocomposite.

Table 1: EDX analysis of (i) TiO_2, (ii) SiO_2, (iii) g-C_3N_4 and (iv) TiO_2/SiO_2/g-C_3N_4.

(i) TiO_2	
Element	Atomic percentage (%)
O	70.04 ± 0.10
Ti	29.96 ± 0.02
Total	100.00
(ii) SiO_2	
Element	Atomic percentage (%)
O	76.52 ± 0.07
Si	23.48 ± 0.03
Total	100.00
(iii) g-C_3N_4	
Element	Atomic percentage (%)
C	38.14 ±0.01
N	61.86 ± 0.07
Total	100.00
(iv) TiO_2/SiO_2/g-C_3N_4	
Element	Atomic percentage (%)
C	74.71 ± 0.03
O	24.66 ± 0.05
Si	0.30 ± 0.00
Ti	0.33 ± 0.00
Total	100.00

Table 2: The diameter of ZOI (mm) for agar well diffusion and disk diffusion, and MIC value (%).

Bacteria	Diameter of ZOI (mm)		MIC (%)
	Agar well diffusion	Disk diffusion	
E. coli	0.0	0.0	0.25
S. aureus	0.0	0.0	1.00

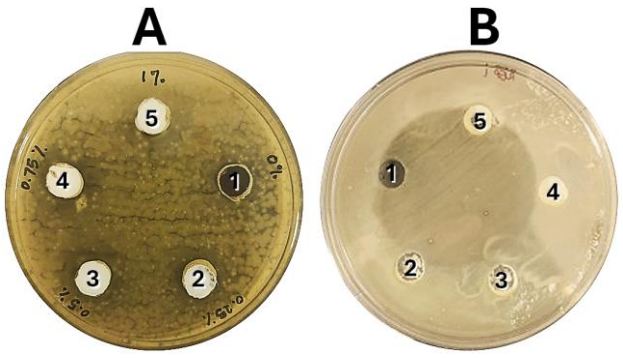

Figure 2: Antibacterial test of TiO_2/SiO_2/g-C_3N_4 nanocomposite with agar well diffusion method: (1) 0% (0.85% saline water), (2) 0.25%, (3) 0.50%, (4) 0.75% and (5) 1.0% against the bacterial strains (A) *E. coli* and (B) *S. aureus*.

microorganisms or applied onto disks placed on inoculated agar plates. Following incubation to allow for microbial growth, the presence of clear zones of inhibition (ZOI) indicated the antibacterial activity of the nanocomposite, reflecting its ability to inhibit or slow down microbial proliferation.

In both the agar well diffusion and disk diffusion tests, no clear zones of inhibition were observed around the TiO_2-SiO_2/g-C_3N_4 wells and disks, as shown in Figures 2 and 3, respectively. This absence of visible inhibition does not necessarily indicate a lack of antibacterial activity but may instead reflect limited diffusion of the nanocomposite through the agar medium under the experimental conditions. Several factors could have contributed to this outcome, including the concentration of the nanocomposite, its physicochemical properties, and its specific interactions with bacterial cells (Younis *et al.*, 2023). Among these, particle size and chemical composition are particularly important, as they directly affect diffusion and ZOI formation. SEM analysis (Figure 1D) revealed that the TiO_2-SiO_2/g-C_3N_4 nanocomposite consists of aggregated particles with estimated sizes ranging from approximately 100 to 300 nm. Given that agar typically possesses pore sizes in the tens of nanometres, such a relatively large particle may have been unable to diffuse effectively through the medium. Supporting this, Osonga *et al.* (2020) demonstrated that spherical silver nanoparticles (AgNPs) with diameters between 9 and 35 nm exhibited size-dependent antifungal activity, with 16 nm particles producing the largest ZOIs. This highlights the critical role of nanoparticle size and morphology in antibacterial performance.

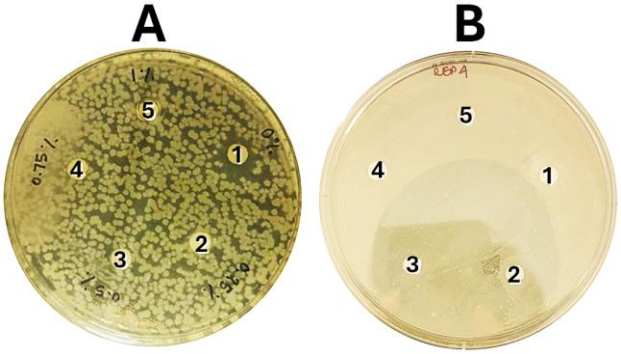

Figure 3: Antibacterial test of TiO_2/SiO_2/g-C_3N_4 nanocomposite with disk diffusion method: (1) 0% (0.85% saline water), (2) 0.25%, (3) 0.50%, (4) 0.75% and (5) 1.0% against the bacterial strains (A) *E. coli* and (B) *S. aureus*.

Additional factors such as poor solubility, limited diffusion capacity, and evaporation dynamics can also influence ZOI formation in agar-based assays (Bubonja-Šonje *et al.*, 2020). In the present study, the nanocomposite's low water solubility likely hindered uniform dispersion and further restricted its mobility within the agar. Moreover, heterogeneous mixtures containing components with differing diffusion rates may yield inconsistent or misleading results. Less polar compounds,

 ISSN (print): 1823-8262, ISSN (online): 2231-7538

Malays. J. Microbiol. Vol 22(1) 2026, pp. 97-105
DOI: http://dx.doi.org/10.21161/mjm.240825

in particular, tend to diffuse slowly through aqueous agar, reducing the likelihood of visible inhibition zones.

The short-lived nature of reactive oxygen species (ROS) generated during TiO_2 photocatalysis adds further complexity. Although ROS are central to antibacterial mechanisms, their lifespans in biological systems range from nanoseconds to seconds, depending on their reactivity and the surrounding antioxidant environment (Dikalov and Harrison, 2014). This transient behaviour limits the spatial and temporal window in which ROS can exert their effects during diffusion-based assays, where physical separation from bacterial cells is common.

Furthermore, the type of agar and its pore size significantly influence the formation of inhibition zones (Yu *et al.*, 2020). For a ZOI to develop, the antibacterial agent must be compatible with the agar matrix and capable of diffusing through it. Agar well and disk diffusion methods provide qualitative assessments of microbial susceptibility based on ZOI dimensions, but they do not distinguish between bactericidal (killing) and bacteriostatic (inhibiting growth) effects (Balouiri *et al.*, 2016; Bubonja-Šonje *et al.*, 2020). These assays are primarily used for preliminary screening, and the absence of a visible ZOI may reflect methodological limitations rather than a lack of antibacterial activity.

To further evaluate the antibacterial efficacy of the TiO_2-SiO_2/g-C_3N_4 nanocomposite, the minimum inhibitory concentration (MIC) was determined using a broth macrodilution assay. MIC is defined as the lowest concentration of an antimicrobial agent that inhibits the visible microbial growth following serial dilution (Loo *et al.*, 2018). In this study, MIC was assessed by measuring sample turbidity before (0 h) and after treatment (24 h) using a spectrophotometer at 600 nm (OD_{600}). Previous studies have employed various approaches to determine MIC by assessing microbial growth inhibition after incubation. For example, Kowalska-Krochmal and Dudek-Wicher (2021) used resazurin, a dye that changes colour in response to microbial metabolic activity, to facilitate the visual determination of microbial growth. While visually straightforward, this method lacks the precision required for quantification. In contrast, spectrophotometric measurement, as used by Arthington-Skaggs *et al.* (2002), offers a more objective and accurate assessment of microbial growth inhibition and is preferred for determining MIC values.

As shown in Table 2, MIC values for the TiO_2-SiO_2/g-C_3N_4 nanocomposite ranged from 0.25% to 1.0%. *Escherichia coli* exhibited an MIC value of 0.25%, while *S. aureus* demonstrated the highest MIC value of 1.0%, indicating that it was less susceptible to TiO_2-SiO_2/g-C_3N_4. This higher MIC value for *S. aureus* may be attributed to the thick peptidoglycan layer in its cell wall, which can act as a barrier to the penetration of antibacterial agents like TiO_2-SiO_2/g-C_3N_4 (Munir and Ahmad, 2022). Additionally, *S. aureus* may possess more efficient efflux pumps that actively expel antibacterial agents such as TiO_2-SiO_2/g-C_3N_4 from the cell, further reducing their effectiveness (Costa *et al.*, 2013).

The discrepancy between the MIC results and the lack of visible ZOIs in agar and disk diffusion assays can be explained by fundamental differences in assay mechanisms. MIC testing is conducted in liquid media, allowing the nanocomposite to remain suspended and in close proximity to bacterial cells. This environment facilitates direct contact and enhances the activity of surface-bound ROS, enabling more effective antibacterial action. Younis *et al.* (2023) similarly reported that TiO_2 nanoparticles exhibited measurable MIC activity against *S. aureus* under ultraviolet (UV) exposure, despite failing to produce visible ZOIs, likely due to poor solubility and restricted diffusion.

In contrast, agar-based diffusion assays such as agar well and disk diffusion rely on the compound's ability to migrate through a solid medium, which is constrained by particle size, solubility, and the short-lived nature of ROS. These factors collectively explain why antibacterial effects were observed in the MIC assay but not in the agar well and disk diffusion tests. Overall, these findings reinforce the notion that photocatalytic antibacterial efficacy depends more on intimate contact and aqueous conditions than on passive diffusion through solid media.

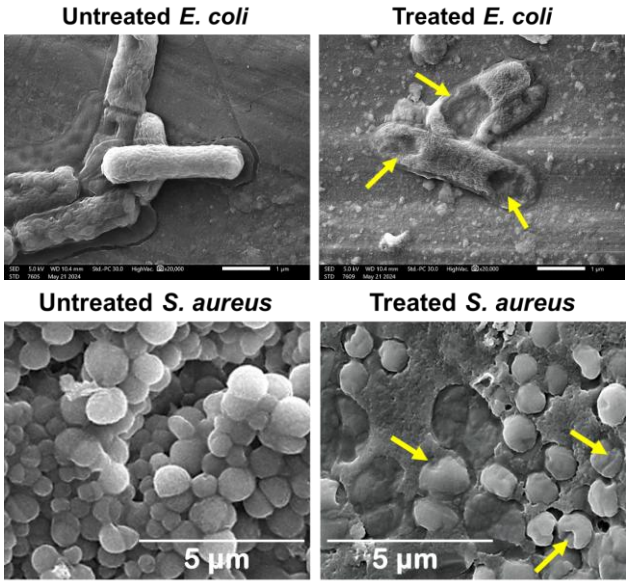

Figure 4: The SEM images of *E. coli* (20000×) and *S. aureus* (5000×) before treatment and after treatment with TiO_2/SiO_2/g-C_3N_4. Arrows indicate cell damage due to cell lysis.

Additional antibacterial investigations were also conducted by analyzing the test bacterial species under SEM to identify any morphological alterations following treatment. For comparison, untreated bacterial species were also analyzed. Figure 4 presents the SEM images of *E. coli* and *S. aureus* before and after treatment with TiO_2-SiO_2/g-C_3N_4 nanocomposite. The *E. coli* samples

 ISSN (print): 1823-8262, ISSN (online): 2231-7538

were imaged at 20,000× magnification, while the *S. aureus* samples were captured at 5,000× magnification.

Figure 4 shows that the cell walls of treated *E. coli* cells were ruptured, displaying visible holes compared to the untreated *E. coli* cells, which appeared smooth and rod-shaped with intact outer membranes. Additionally, some portions of the membrane were lysed, and cellular debris, marked by arrows in the SEM images were observed around the cells due to membrane leakage.

Untreated *S. aureus* cells exhibited the characteristic spherical shape, appearing smooth, intact, and uniformly clustered with consistent size distribution. No structural damage or surface irregularities were evident. In contrast, treated *S. aureus* cells showed significant morphological alterations, including irregular shapes, disrupted surfaces, and visible nanocomposite adherence. These deformations suggest cell wall disintegration and lysis, indicating that the TiO_2-SiO_2/g-C_3N_4 nanocomposite effectively compromised bacterial integrity in both Gram-negative and Gram-positive strains.

The observed membrane damage is attributed to the photocatalytic activity of the TiO_2-SiO_2/g-C_3N_4 nanocomposite. This composite material combines TiO_2, SiO_2, and g-C_3N_4, each contributing unique properties. TiO_2 provides robust photocatalytic activity under UV light, SiO_2 enhances charge separation, and g-C_3N_4 extends activity into the visible light spectrum. The synergistic combination results in a composite with superior photocatalytic performance compared to the individual materials (Yu *et al.*, 2020). The photocatalytic activity of the TiO_2-SiO_2/g-C_3N_4 nanocomposite generates ROS, including hydroxyl radicals (•OH) and superoxide anions ($O_2^{\bullet-}$), which degrade organic compounds and damage microbial structures (Yu *et al.*, 2020; Zheng *et al.*, 2023).

ROS exert antibacterial effects through oxidative stress, damaging key cellular components. They penetrate bacterial cells and induce DNA oxidation, protein carbonylation, and lipid peroxidation (Juan *et al.*, 2021; Ayala *et al.*, 2014). Lipid peroxidation compromises membrane integrity, increasing permeability and disrupting barrier function (Demirel *et al.*, 2018; Hirata *et al.*, 2023). This cascade of damage leads to cell lysis and morphological collapse (Rice and Bayles, 2008; González-Jiménez *et al.*, 2023).

The unique nanostructure of TiO_2-SiO_2/g-C_3N_4 nanocomposite enhances its antibacterial efficacy by increasing the surface area and physical interactions with bacterial cells. The irregular shape and rough surface of the nanocomposite particles, as depicted in Figure 1(D), enhance antibacterial efficacy by providing a larger contact area with bacterial membranes. This facilitates stronger localized ROS generation and mechanical stress, both of which contribute to membrane disruption and cell death (Wang *et al.*, 2017; Liu *et al.*, 2021).

Although only two bacterial species were tested, they represent both Gram-negative (*E. coli*) and Gram-positive (*S. aureus*) classes, offering a foundational understanding of the nanocomposite's antibacterial potential. The observed differences in MIC values and morphological alterations between these strains provide meaningful insight into its spectrum of activity. The synergistic interactions among TiO_2, SiO_2 and g-C_3N_4 enhance the nanocomposite's photocatalytic performance and enable a multi-modal mechanism of action, further underscoring its versatility. Notably, its antibacterial efficacy is optimized in moist environments, where water facilitates ROS generation and surface-mediated antimicrobial activity. Future studies will expand the range of tested microorganisms, including antibiotic-resistant strains, to further validate and broaden the applicability of these findings.

CONCLUSION

The TiO_2-SiO_2/g-C_3N_4 nanocomposite exhibited measurable antibacterial activity against *E. coli* and *S. aureus*, particularly under conditions that promote close contact and aqueous dispersion, as demonstrated by MIC results. These findings suggest that TiO_2-SiO_2/g-C_3N_4 nanocomposite could contribute meaningfully to the development of advanced antibacterial systems, particularly in applications such as wastewater treatment, where direct contact and aqueous environments prevail.

ACKNOWLEDGEMENTS

This study was financially supported by the VC-High Impact Research Grant [UNI/F07/VC-HIRG/85507/P10-02/2022].

REFERENCES

Al-Abri, M., Al-Ghafri, B., Bora, T., Dobretsov, S., Dutta, J., Castelletto, S. *et al.* (2019). Chlorination disadvantages and alternative routes for biofouling control in reverse osmosis desalination. *Nature Partner Journals Clean Water* **2(1), 1-16.**

Arthington-Skaggs, B. A., Lee-Yang, W., Ciblak, M. A., Frade, J. P., Brandt, M. E., Hajjeh, R. A. *et al.* (2002). Comparison of visual and spectrophotometric methods of broth microdilution MIC end point determination and evaluation of a sterol quantitation method for *in vitro* susceptibility testing of fluconazole and itraconazole against trailing and nontrailing *Candida* isolates. *Antimicrobial Agents and Chemotherapy* **46(8), 2477-2481.**

Ayala, A., Muñoz, M. F. and Argüelles, S. (2014). Lipid peroxidation: Production, metabolism, and, signaling mechanisms of malondialdehyde and 4-hydroxy-2 nonenal. *Oxidative Medicine and Cellular Longevity* **2014, Article ID 360438.**

Balouiri, M., Sadiki, M. and Ibnsouda, S. K. (2016). Methods for *in vitro* evaluating antimicrobial activity: A review. *Journal of Pharmaceutical Analysis* **6(2), 71-79.**

Bauer, A. W., Kirby, W. M., Sherris, J. C. and Turck, M. (1966). Antibiotic susceptibility testing by a standardized single disk method. *American Journal of Clinical Pathology* **45(4), 493-496.**

 ISSN (print): 1823-8262, ISSN (online): 2231-7538

Bubonja-Šonje, M., Knežević, S. and Abram, M. (2020). Challenges to antimicrobial susceptibility testing of plant-derived polyphenolic compounds. *Archives of Industrial Hygiene and Toxicology* **71(4), 300-311.**

Byrne, J. A., Dunlop, P. S. M., Hamilton, J. W. J., Fernández-Ibáñez, P., Polo-López, I., Sharma, P. K. and Vennard, A. S. M. (2015). A review of heterogeneous photocatalysis for water and surface disinfection. *Molecules* **20(4), 5574-5615.**

Clinical and Laboratory Standards Institute (CLSI). (2015). Methods for dilution antimicrobial susceptibility tests for bacteria that grow aerobically; Approved standard-tenth edition. *CLSI document M07-A10* **35(2), 15-47.**

Costa, S. S., Viveiros, M., Amaral, L. and Couto, I. (2013). Multidrug efflux pumps in *Staphylococcus aureus*: An update. *The Open Microbiology Journal* **7, 59-71.**

Demirel, C. S. U., Birben, C. N. and Bekbolet, M. (2018). A comprehensive review on the use of second generation TiO_2 photocatalysts: Microorganism inactivation. *Chemosphere* **211, 420-448.**

Dikalov, S. I., and Harrison, D. G. (2014). Methods for detection of mitochondrial and cellular reactive oxygen species. *Antioxidants and Redox Signaling* **20(2), 372-382.**

Dong, H., Zeng, G., Tang, L., Fan, C., Zhang, C., He, X. *et al.* (2015). An overview on limitations of TiO_2-based particles for photocatalytic degradation of organic pollutants and the corresponding countermeasures. *Water Research* **79, 128-146.**

Edokpayi, J., Rogawski, E., Kahler, D., Hill, C., Reynolds, C., Nyathi, E. *et al.* (2018). Challenges to sustainable safe drinking water: A case study of water quality and use across seasons in rural communities in Limpopo Province, South Africa. *Water* **10(2), 159.**

Etacheri, V., Valentin, C. D., Schneider, J., Bahnemann, D. and Pillai, S. C. (2015). Visible-light activation of TiO_2 photocatalysts: Advances in theory and experiments. *Journal of Photochemistry and Photobiology C: Photochemistry Reviews* **25, 1-29.**

González-Jiménez, I., Perlin, D. S. and Shor, E. (2023). Reactive oxidant species induced by antifungal drugs: Identity, origins, functions, and connection to stress-induced cell death. *Frontiers in Cellular and Infection Microbiology* **13, 1276406.**

Griffiths, J. K. (2008). Waterborne diseases. *International Encyclopedia of Public Health* **551-563.**

Gupta, V., Shekhawat, S. S., Kulshreshtha, N. M. and Gupta, A. B. (2022). A systematic review on chlorine tolerance among bacteria and standardization of their assessment protocol in wastewater. *Water Science and Technology* **86(2), 261-291.**

Guyett, P. C., Chew, D., Azevedo, V., Blennerhassett, L. C., Rosca, C. and Tomlinson, E. (2024). Optimizing SEM-EDX for fast, high-quality and non-destructive elemental analysis of glass. *Journal of Analytical Atomic Spectrometry* **39(10), 2565-2579.**

Hirata, Y., Cai, R., Volchuk, A., Steinberg, B. E., Saito, Y., Matsuzawa, A. *et al.* (2023). Lipid peroxidation increases membrane tension, Piezo1 gating, and cation permeability to execute ferroptosis. *Current Biology* **33(7), 1282-1294.e5.**

Juan, C. A., Pérez de la Lastra, J. M., Plou, F. J. and Pérez-Lebeña, E. (2021). The chemistry of reactive oxygen species (ROS) revisited: Outlining their role in biological macromolecules (DNA, lipids and proteins) and induced pathologies. *International Journal of Molecular Sciences* **22(9), 4642.**

Kanakaraju, D., Abdul, M. A. and Chin, L. Y. (2021). TiO_2/PKSAC functionalized with Fe_3O_4 for efficient concurrent removal of heavy metal ions from water. *Colloid and Interface Science Communications* **40, 100353.**

Kowalska-Krochmal, B. and Dudek-Wicher, R. (2021). The minimum inhibitory concentration of antibiotics: Methods, interpretation, clinical relevance. *Pathogens* **10(2), 165.**

Kumar, S., Karthikeyan, S. and Lee, A. F. (2018). g-C_3N_4-based nanomaterials for visible light-driven photocatalysis. *Catalysts* **8(2), 74.**

Liu, N., Ming, J., Sharma, A., Sun, X., Naoki, K., Chen, G. *et al.* (2021). Sustainable photocatalytic disinfection of four representative pathogenic bacteria isolated from real water environment by immobilized TiO_2-based composite and its mechanism. *Chemical Engineering Journal* **426, 131217.**

Loo, Y. Y., Rukayadi, Y., Nor-Khaizura, M., Kuan, C. H., Chieng, B. W., Nishibuchi, M. *et al.* (2018). *In vitro* antimicrobial activity of green synthesized silver nanoparticles against selected Gram-negative foodborne pathogens. *Frontiers in Microbiology* **9, 1555.**

Magana-Arachchi, D. N. and Wanigatunge, R. P. (2020). Ubiquitous waterborne pathogens. *Waterborne Pathogens* **2020, 15-42.**

Moma, J. and Baloyi, J. (2018). Modified titanium dioxide for photocatalytic applications. *In:* Photocatalyst-Applications and Attributes. Khan, S. B. and Akhtar, K. (eds.). IntechOpen, London, United Kingdom. **pp. 1-20**.

Munir, M. U. and Ahmad, M. M. (2022). Nanomaterials aiming to tackle antibiotic-resistant bacteria. *Pharmaceutics* **14(3), 582.**

Nielsen, A. M., Garcia, L. A. T., Silva, K. J. S., Sabogal-Paz, L. P., Hincapié, M. M., Montoya, L. J. *et al.* (2022). Chlorination for low-cost household water disinfection - A critical review and status in three Latin American countries. *International Journal of Hygiene and Environmental Health* **244, 114004.**

Osonga, F. J., Akgul, A., Yazgan, I., Akgul, A., Eshun, G. B., Sakhaee, L. *et al.* (2020). Size and shape-dependent antimicrobial activities of silver and gold nanoparticles: A model study as potential fungicides. *Molecules* **25(11), 2682.**

Qadafi, M., Rosmalina, R. T., Pitoi, M. M. and Wulan, D. R. (2023). Chlorination disinfection by-products in Southeast Asia: A review on potential precursor, formation, toxicity assessment, and removal technologies. *Chemosphere* **316, 137817.**

Rades, S., Hodoroaba, V., Salge, T., Wirth, T., Lobera, M. P., Labrador, R. H. *et al.* (2014). High-resolution imaging with SEM/T-SEM, EDX and SAM as a combined methodical approach for morphological and elemental analyses of single engineered nanoparticles. *Royal Society of Chemistry* **4, 49577-49587.**

Rice, K. C., and Bayles, K. W. (2008). Molecular control of bacterial death and lysis. *Microbiology and Molecular Biology Reviews* **72(1), 85-109.**

Sareshkeh, A. T, Dorraji, M. S. S., Karami, Z., Shahmoradi, S., Fekri, E., Daneshvar, H. *et al.* (2023). Preparation of high-crystalline and non-metal modified g-C_3N_4 for improving ultrasound-accelerated white-LED-light-driven photocatalytic performances. *Scientific Reports* **13, 15079.**

Singh, P., Gupta, S. K., Guldhe, A., Rawat, I. and Bux, F. (2015). Microalgae isolation and basic culturing techniques. *In:* Handbook of marine microalgae. Kim, S.-K. (ed.). Academic Press, New York. **pp. 43-54.**

Wacogne, B., Podevin, M. B., Vaccari, N., Koubevi, C., Codjiová, C., Gutierrez, E. *et al.* (2024). Concentration vs. optical density of ESKAPEE bacteria: A method to determine the optimum measurement wavelength. *Sensors* **24(24), 8160.**

Wang, L., Hu, C. and Shao, L. (2017). The antimicrobial activity of nanoparticles: Present situation and prospects for the future. *International Journal of Nanomedicine* **12, 1227-1249.**

Wardani, D. A. P., Hariyanto, B., Kurniawati, N., Har, N. P., Darmawan, N. and Irzaman, I. (2023). Functional groups, band gap energy, and morphology properties of annealed silicon dioxide (SiO_2). *Egyptian Journal of* Chemistry **66(3), 529-535.**

Wu, Y., Chen, S., Zhao, J., Yue, X., Deng, W., Li, Y. *et al.* (2016). Mesoporous graphitic carbon nitride and carbon-TiO_2 hybrid composite photocatalysts with enhanced photocatalytic activity under visible light irradiation. *Journal of Environmental Chemical Engineering* **4(1), 797-807.**

Younis, A. B., Milosavljevic, V., Fialova, T., Smerkova, K., Michalkova, H., Svec, P. *et al.* (2023). Synthesis and characterization of TiO_2 nanoparticles combined with geraniol and their synergistic antibacterial activity. *BMC Microbiology* **23(1), 207.**

Yu, Y., Xu, W., Fang, J., Chen, D., Pan, T., Feng, W. *et al.* (2020). Soft-template assisted construction of superstructure TiO_2/SiO_2/g-C_3N_4 hybrid as efficient visible-light photocatalysts to degrade berberine in seawater via an adsorption-photocatalysis synergy and mechanism insight. *Applied Catalysis B: Environmental and Energy* **268, 118751.**

Zheng, M., Lin, Y. and Liu, S. (2023). TiO_2@g-C_3N_4/SiO_2 with superior visible light degradation of formaldehyde for indoor humidity control coatings. *Materials Today Sustainability* **24, 100496.**

 ISSN (print): 1823-8262, ISSN (online): 2231-7538